

Soil analysis using a 2" Nal gamma detector

Rebekah Aguilar, Patrick Powers, Nina Abramzon, and P. B. Siegel

Citation: *American Journal of Physics* **89**, 647 (2021); doi: 10.1119/10.0003490

View online: <https://doi.org/10.1119/10.0003490>

View Table of Contents: <https://aapt.scitation.org/toc/ajp/89/6>

Published by the [American Association of Physics Teachers](#)

ARTICLES YOU MAY BE INTERESTED IN

[Euler's rigid rotators, Jacobi elliptic functions, and the Dzhanibekov or tennis racket effect](#)
American Journal of Physics **89**, 349 (2021); <https://doi.org/10.1119/10.0003372>

[Acoustic levitation and the acoustic radiation force](#)
American Journal of Physics **89**, 383 (2021); <https://doi.org/10.1119/10.0002764>

[Plasma generation by household microwave oven for surface modification and other emerging applications](#)
American Journal of Physics **89**, 372 (2021); <https://doi.org/10.1119/10.0002706>

[Tesla's fluidic diode and the electronic-hydraulic analogy](#)
American Journal of Physics **89**, 393 (2021); <https://doi.org/10.1119/10.0003395>

[Fréedericksz transition on air](#)
American Journal of Physics **89**, 603 (2021); <https://doi.org/10.1119/10.0003350>

[Gravitational waves physics using Fermi coordinates: A new teaching perspective](#)
American Journal of Physics **89**, 639 (2021); <https://doi.org/10.1119/10.0003513>



Advance your teaching and career
as a member of **AAPT**

LEARN MORE





INSTRUCTIONAL LABORATORIES AND DEMONSTRATIONS

John Essick, *Editor*

Department of Physics, Reed College, Portland, OR 97202

Articles in this section deal with new ideas and techniques for instructional laboratory experiments, for demonstrations, and for equipment that can be used in either. Although these facets of instruction also appear in regular articles, this section is for papers that primarily focus on equipment, materials, and how they are used in instruction.

Manuscripts should be submitted using the web-based system that can be accessed via the American Journal of Physics home page, ajp.aapt.org, and will be forwarded to the IL&D editor for consideration.

Soil analysis using a 2" NaI gamma detector

Rebekah Aguilar, Patrick Powers, Nina Abramzon, and P. B. Siegel^{a)}

Department of Physics and Astronomy, California State Polytechnic University Pomona, Pomona, California 91768

(Received 29 April 2020; accepted 21 January 2021)

We describe an undergraduate physics laboratory experiment that uses a 2-inch diameter NaI gamma detector to measure natural radiation in soils. Students first calibrate the detector for the source-detector geometry, energy-dependent detection efficiency, and sample self-absorption. Then, the activity of the ^{238}U and ^{232}Th decay series, as well as the activity of ^{40}K in the soil, are measured. The results are comparable in accuracy to those obtained using a high-resolution germanium gamma detector. © 2021 Published under an exclusive license by American Association of Physics Teachers.

<https://doi.org/10.1119/10.0003490>

I. INTRODUCTION

Gamma spectroscopy is a fairly common laboratory exercise in the undergraduate physics curriculum. In a previous article, we described an experiment to measure gamma radiation from environmental samples using a high-resolution germanium detector.¹ The experiment has been a favorite for our students, who we have found are curious about the amount of radiation in their environment and enjoy testing different soils in their neighborhoods. However, due to their high cost, high-resolution gamma detectors are not typically a part of the undergraduate instructional laboratory. More common are medium-size 2-inch diameter sodium iodide (NaI) gamma detectors. As a comparison between these two types of detectors, the resolution for the 662 keV photopeak of ^{137}Cs is 6.6% for our NaI detector and 0.19% for our germanium detector. Unfortunately, due to the lower resolution of the NaI detector, many of the gammas emitted from the naturally found isotopes of the ^{238}U and the ^{232}Th series cannot be resolved, and the methods used in Ref. 1 cannot be applied. However, as we will show, using a 2-inch NaI gamma detector, one can do a meaningful physics laboratory experiment, where the students measure the main sources of terrestrial gamma radiation in their environment, i.e., ^{40}K , the ^{238}U and the ^{232}Th decay series, and learn how to calibrate the detector for efficiency and sample self-absorption.

There are two features that make the analysis possible. First, there is an emitted gamma from each of the decay series that is resolvable with the NaI detector. For the ^{238}U series, the isotope ^{214}Bi emits a gamma with energy 1764 keV, while for the ^{232}Th series, the isotope ^{208}Tl emits a gamma with energy 2614 keV. The 1461 keV gamma from

^{40}K is also clearly observable in the spectrum. In Fig. 1, we show the gamma spectra acquired from our 2-inch NaI detector with and without a soil sample present. Each of the three peaks are labeled in the figure and can be fitted by Gaussian functions to determine the count rate. Second, the energy dependence of the detection efficiency and self-absorption by the sample obey an approximate power law relationship between 511 and 2614 keV. This empirically obtained relation enables one to compare count rates of gammas with different energies.¹

The relationship between the gamma count rate C and the isotope activity A is given by $C = AYS^S(E_\gamma)\epsilon(E_\gamma)$, where Y is the gamma yield, $\epsilon(E_\gamma)$ is the detector efficiency, and $S^S(E_\gamma)$ is the self-absorption factor for sample "s." The gamma yield is the probability that a gamma of energy E_γ is emitted when the isotope undergoes a decay. The efficiency $\epsilon(E_\gamma)$ depends on the size of the detector, the detector-source geometry, and the energy E_γ of the gamma. The self-absorption factor $S^S(E_\gamma)$ corrects for gammas being absorbed in the sample and not reaching the detector; $S^S(E_\gamma)$ depends on the energy E_γ of the gamma as well as the density, size and shape of the soil. To a good approximation, the energy dependence of the product $S^S(E_\gamma)\epsilon(E_\gamma)$ follows a power law relationship,¹ $S^S\epsilon \propto E_\gamma^b$, which allows one to relate the count rate to the isotope activity via $C \propto AYE_\gamma^b$. In order to have the proportionality constant to be unitless, we express this relationship as

$$C = AYS_{1461}^S \epsilon_{1461} \left(\frac{E_\gamma}{1461 \text{ keV}} \right)^b, \quad (1)$$

where we have defined $S_{1461}^S \equiv S^S(1461 \text{ keV})$ and $\epsilon_{1461} \equiv \epsilon(1461 \text{ keV})$. The constants ϵ_{1461} , S_{1461}^S , Y , and b are unitless. The quantities C and A have the dimensions time^{-1} and

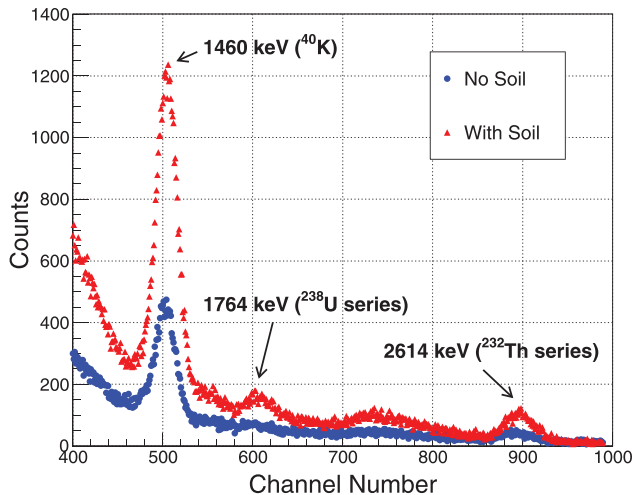


Fig. 1. Soil spectrum, plotted as solid triangles, and background spectrum, plotted as solid circles. The background spectra is a reading without the soil present. The collection time was 24 h for both spectra.

E_γ has units of keV. The product $S_{1461}^s \epsilon_{1461}$ is the probability of detecting a 1461 keV gamma emitted by the soil sample, averaged throughout the soil volume. We have chosen 1461 keV since we will use a KCl sample with the same detector-source geometry as the soil to determine the product $S_{1461}^{KCl} \epsilon_{1461}$.

In Sec. II, we describe a classroom experiment in which a soil sample is characterized using the NaI detector. We will show results for two different soil samples that have different densities: a soil sample from a backyard near our university, and a more dense desert soil from Nevada.

II. CLASSROOM EXPERIMENT

The classroom experiment we have developed takes place over two three-hour laboratory sessions. In the first session, students calibrate their NaI detector, i.e., determine b and $S_{1461}^s \epsilon_{1461}$ in Eq. (1). A week later in the second session, the students analyze the soil samples. To carry out the analysis, students use the following equipment: A 2" NaI gamma detector connected to a multichannel analyzer is used to collect the gamma spectra.² To verify the power law relation of Eq. (1) and to estimate the exponent b , we use three common isotope disk sources: ^{207}Bi , ^{22}Na , and ^{60}Co . The disk sources are essentially point sources of radiation. They each have an activity of around 1 μCi and do not need to be calibrated. Identical containers are used for the soil samples and a KCl calibration sample. Each container has a volume of around

Table I. Isotopes and their corresponding gamma energies, E_γ , and yields Y for the three disk sources. The values are from Ref. 3.

Isotope	E_γ (keV)	Yield
^{207}Bi	570	0.977
...	1064	0.745
...	1770	0.0687
^{22}Na	511	1.80
...	1275	1.0
^{60}Co	1173	1.0
...	1332	1.0

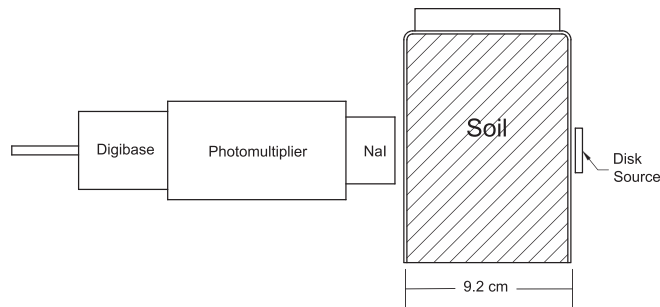


Fig. 2. Picture of a student's setup with soil and disk source. The NaI crystal and the soil sample are drawn to scale. The source is the small disk behind the soil.

1000 cm^3 (32 oz), and the containers are filled with the same volume of material.

For the first session, each group of (two or three) students has its own NaI detector, soil sample, and KCl calibration sample. We have enough NaI detectors to handle eight student groups at once. The three disk sources are shared among the groups. We run the experiments using an inquiry-based approach, which leads to active classroom discussions and sharing of ideas.

A. Determining the exponent b

The students' first task is to determine the energy dependence of the product $S^s(E_\gamma)\epsilon(E_\gamma)$. As shown in Ref. 1, a nice method for determining $S^s(E_\gamma)\epsilon(E_\gamma)$ is to examine the count rate divided by the yield, i.e., C/Y , for gammas emitted from isotopes that emit more than one gamma and have the same detector-source geometry.

To compensate for the lower resolution of the NaI detector, the students use small disk sources to examine the dependence of $S^s(E_\gamma)\epsilon(E_\gamma)$ on the energy E_γ and to estimate the exponent b . For this analysis, each source needs to emit two or more gammas. The most common sources available for this purpose are ^{207}Bi , ^{22}Na , and ^{60}Co , which emit three, two, and two gammas, respectively. The gamma energies and yields for these disk sources are listed in Table I. Data are collected as follows. First, the soil sample is placed up against the detector. Next, a reading is taken with one of the sources behind the soil. The soil is then removed, keeping the source at the same location, and another reading is taken. A diagram of the student setup using the disk sources is shown in Fig. 2. In each case, sufficient counts can be obtained in 10 – 15 min. Six spectra are acquired in all: each of the three sources without the soil attenuation and each source with the soil attenuation.

For each source D, we use the following formula for the count rate $C_D(E_\gamma)$ as a function of the gamma energy E_γ :

$$C_D(E_\gamma) = C_{D1461Y1} Y_\gamma \left(\frac{E_\gamma}{1461 \text{ keV}} \right)^b, \quad (2)$$

$$\frac{C_D(E_\gamma)}{Y_\gamma} = C_{D1461Y1} \left(\frac{E_\gamma}{1461 \text{ keV}} \right)^b, \quad (3)$$

where $C_{D1461Y1}$ and Y_γ are constants for each source D. Y_γ is the gamma yield, and $C_{D1461Y1}$ is the count rate that would be measured if the source D emitted a gamma with energy 1461 keV and yield 1. We use this ansatz to assist in

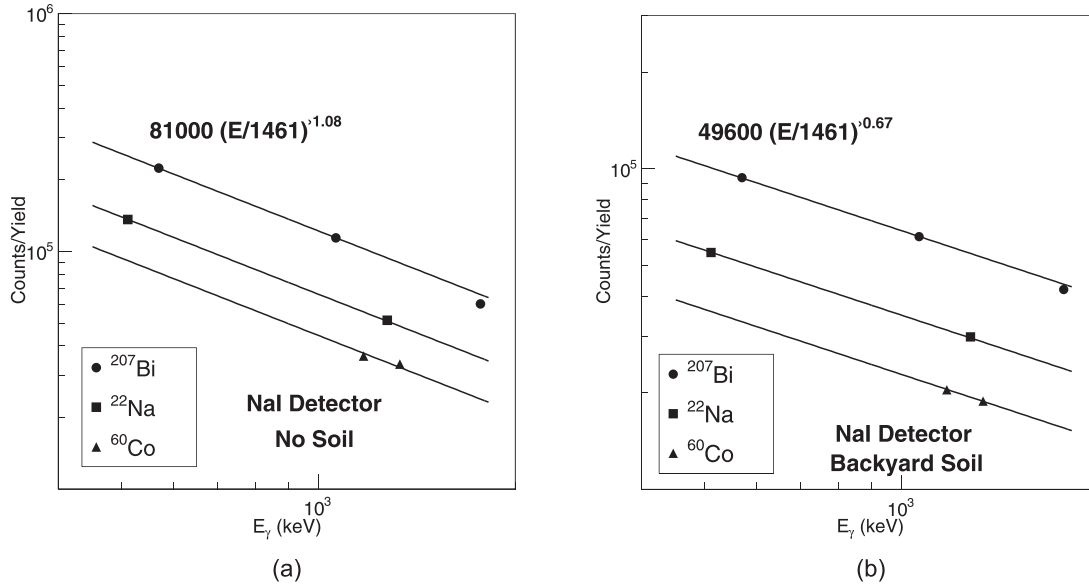


Fig. 3. (a) Graph of C_D/Y for the disk sources without the soil. The log-log graph, with a common slope of $b_0 = -1.08$ for each isotope, demonstrates that $\epsilon(E_\gamma)$ is well approximated by a power law function in the energy range $511 \rightarrow 1770$ keV. The equation is for the ^{207}Bi source. (b) Graph of C_D/Y for the disk sources with soil attenuation. The common slope b_s in this case is -0.67 . Note that the value of C_{Bi1461Y1} without the soil is 81 000 counts and with the soil present is 49 600 counts, resulting in a value of f of 0.61 for the backyard soil sample.

measuring the attenuation of a 1461 keV gamma through the soil (see Appendix B). The students first measure the counts C_D from the gammas emitted from each of the three disk sources without the soil attenuation. The seven values of C_D/Y_γ are fit with four parameters (the common exponent b , C_{Bi1461Y1} , C_{Na1461Y1} , and C_{Co1461Y1}) using a linear regression⁶ method or a weighted χ^2 search routine.^{4,7} A typical graph of C_D/Y without soil attenuation is shown in Fig. 3(a). As can be seen from the graph, the measurements without the soil present demonstrate that $\epsilon(E_\gamma)$ is well approximated by a power law function in the energy range $511 \rightarrow 1770$ keV.

The next task is to get an estimate of the exponent b for the soil sample. Absorption of the radiation in the soil sample is an important factor, since lower energy gammas are absorbed more than high energy ones. To examine the degree of self-absorption, the students analyze C_D/Y for the three spectra with the soil attenuation. In Fig. 3(b), we display a typical result for C_D/Y with the soil between source and detector. As one can see, remarkably $S^s(E_\gamma)\epsilon(E_\gamma)$ also obeys a power-law function even after the radiation travels through the soil. By comparing the two graphs, one sees that the soil shields out around half of the gamma radiation at 511 keV, but only around a third at 1770 keV. The exponent b changes from -1.08 to -0.67 due to self-absorption. The correct value for b lies somewhere between these two extremes. For simplicity, one can take an average of the two values: $b = (-1.08 - 0.67)/2 \approx -0.88$. In Appendix A, we

estimate the accuracy of this simple approach and discuss other options. We find that the amount of self-absorption and hence the value of b depends mainly on the density of the soil sample. In Table II, we list the values of b for the backyard and desert soils.

B. Determining the efficiency constant ϵ_{1461}

To determine the calibration product $S_{1461}^s \epsilon_{1461}$, students measure a sample of potassium chloride KCl in an identical container filled with the same volume as the soil sample. Using the natural abundance of ^{40}K , which is 0.000117, the activity of the KCl sample is calculated. The product $S_{1461}^{\text{KCl}} \epsilon_{1461}$ can be determined by a measurement of the count rate. For example, our KCl sample has a mass of 863 g. One first determines the number of moles in the sample from the molar mass of KCl (74.55 g/mole). Since each molecule contains one potassium atom, the number of ^{40}K nuclei is $N_{\text{K40}} \approx (863/74.55)(6.02 \times 10^{23})(0.000117) \approx 8.15 \times 10^{20}$ nuclei. The activity of ^{40}K in the sample is determined from $A_{\text{K40}} = N_{\text{K40}} \ln(2)/\tau$, where τ is the half life of 1.248×10^9 years. In our case, $A_{\text{K40}} \approx 14360$ Bq. The gamma yield for ^{40}K to emit a 1461 keV gamma is 0.1069. Thus, the rate of 1461 keV gammas emitted by our KCl sample is around 1535 gammas/s. Students record the KCl data for 30 min as well as an ambient background spectrum for 30 min. A recent count rate minus background for the 1461 keV photopeak of the KCl sample was 9018 counts/(30 min), which gives $S_{1461}^{\text{KCl}} \epsilon_{1461} \approx 0.00326$. However, for our soil measurements, we need the value of $S_{1461}^s \epsilon_{1461}$. Since the density of the KCl sample is different than the soil sample, there is a small difference between S_{1461}^s and S_{1461}^{KCl} . In Appendix B, we estimate this difference in self-absorption between the soil and the KCl sample at $E_\gamma = 1461$ keV. For the backyard sample, we have $S_{1461}^{\text{backyard}}/S_{1461}^{\text{KCl}} \approx 0.93$. With this value, we obtain a value for $S_{1461}^{\text{backyard}} \epsilon_{1461} \approx 0.93(0.00326) \approx 0.00303$ with a statistical error of around 1%. The calibration of the detector is

Table II. Calibration parameters b and $S_{1461}^s \epsilon_{1461}$ for the two soil samples.

Parameter	Backyard Soil (1300 g)	Desert Soil (1790 g)
b_0 (no soil)	-1.08	-1.08
b_s (with soil)	-0.67	-0.51
b_{ave}	-0.88	-0.80
b [Eq. (A2)]	-0.97	0.93
$S_{1461}^s \epsilon_{1461}$	0.00303	0.00267



Fig. 4. Soil measurement setup. When the spectrum is collected, bricks are added to cover up the sample and detector. During collection, the sample and detector are completely shielded by 5 cm of lead.

now complete. For the backyard soil, the count rate C is related to the activity A in the soil by

$$C = AY(0.00303) \left(\frac{E_\gamma}{1461 \text{ keV}} \right)^{-0.88}. \quad (4)$$

In Table II, we compare the calibration parameters for the two soils to show the effect of density on b and $S_{1461}^S \epsilon_{1461}$.

C. Measuring the soil sample

Once the calibration is done, students can analyze the soil sample. Since this sample hopefully has only a small amount of gamma radiation, one needs to collect data for a long time with exceptional shielding. The setup for the soil sample measurement is shown in Fig. 4. We have only one such experimental station since it is not practical to have more than one heavily shielded detector setup. It is absolutely critical to have good shielding from background radiation when measuring the soil sample. The shielding shown in Fig. 4 results in a signal (soil) to background (no soil) ratio of 3.5 for the 1461 keV peak. During the one week between lab sessions, gamma spectra are collected by the instructor for 24 h for each soil sample as well as one background spectrum. In order to have the 2614 keV gamma fit into the spectrum, we needed to lower the amplifier gain and high voltage setting of the photomultiplier from those used by students for the disk source and KCl measurements. We lowered the amplifier gain from 1.2 to 0.55 and the high voltage from 900 V to 690 V. It is easier for students to measure the disk sources if the highest energy of 1770 keV is around channel number 850 so that the photopeaks are spread out across the entire 1024 channels of the multichannel analyzer. We have

Table IV. Results of the Backyard soil analysis. The activities A are calculated using Eq. (4). The errors listed are statistical only. Note that the counts with the soil are around three times background (without soil).

Isotope	E_γ (keV)	Soil (counts/24 h)	No-Soil (counts/24 h)	A (Bq)	Per Mass
^{40}K	1461	35150 ± 190	9254 ± 96	925 ± 9	2.2% K by wt
^{214}Bi (^{238}U series)	1764.5	1080 ± 33	330 ± 18	$A_{\text{U}238} = 22 \pm 2$	17 Bq/kg
^{208}Tl (^{232}Th series)	2614.5	3398 ± 58	1078 ± 33	$A_{\text{Th}232} = 41 \pm 2$	31 Bq/kg

Table III. Isotopes and their corresponding gamma energies, E_γ , and yields for the soil analysis. The data are from Ref. 3. Note for ^{208}Tl we list the effective yield as discussed in the text.

Isotope	E_γ (keV)	Yield
^{40}K	1461	0.1069
^{214}Bi (^{238}U series)	1729.6	0.0288
...	1764.5	0.153
...	1847.4	0.0203
^{208}Tl (^{232}Th series)	2614.5	$0.3594(0.9975) \approx 0.3585$

checked that the two settings result in the same values for the calibration parameters b and $S_{1461}^{\text{KCl}} \epsilon_{1461}$.

Students determine the area under the three photopeaks of Table III using a Gaussian plus background function as in Ref. 5 for both the soil spectra and the no-soil spectra. After subtracting the count rate of the no-soil photopeak from the soil photopeak, the calibration given in Eq. (1) is used to determine the activity of radioactive isotopes in the soil in units of Bq and Bq/kg. The percent of potassium by weight in the soil is also determined. In Table IV, we display data for the backyard soil sample, with statistical errors, from a student experiment. Since the decay series are in secular equilibrium, the activities listed are the activities of ^{238}U and ^{232}Th .

III. DISCUSSION

Although the statistical errors are relatively small, there are systematic uncertainties that can be important. Below, we mention some of these errors and comment on other aspects of the experiment. Many of these ideas are brought up in our classroom discussions.

- (1) The exponent b is a critical parameter in the soil analysis. The measurements to estimate b use disk sources that have gammas with energies between 511 and 1770 keV. However, the three gammas that are measured in the soil analysis have energies of 1461, 1764, and 2614 keV, and calibration is done at the energy 1461 keV. For the ^{232}Th series measurement at 2614 keV, we need to extrapolate out to 2614 keV and errors in b can become important. Since 1764 keV is only around 20% larger than 1461 keV, uncertainties in the exponent b do not affect the ratio $(S^S(1764)\epsilon(1764))/(S^S(1461)\epsilon(1461))$ significantly. The effect will be larger for the relative efficiency ratio $(S^S(2614)\epsilon(2614))/(S^S(1461)\epsilon(1461))$ since $2614/1461 \approx 1.79$. In Appendix A, we determined that b should lie between b_{ave} and b [Eq. (A2)]. For both soils, this range is 10% of b_{ave} . Suppose our estimate for b is off by 10%, say -0.9 instead of -1.0 . Then the ratio $(S^S(2614)\epsilon(2614))/(S^S(1461)\epsilon(1461))$ would have an error of $(1.79^{-1} - 1.79^{-0.9})/1.79^{-1} \approx 0.06$ or 6%.

- (2) If one is interested in the activities of ^{238}U and ^{232}Th from measurements of the isotopes ^{214}Bi and ^{208}Tl , the respective series must be in secular equilibrium and the appropriate yield must be used. In the ^{238}U decay series, the isotope ^{222}Rn , which is an inert gas with a half life around 3.8 days, comes before ^{214}Bi . In order to keep the gas from escaping the soil, as it does in nature, one needs to ensure that the container is “air tight” for few half-lives of ^{222}Rn .¹ For the ^{232}Th decay series, ^{220}Rn has a half life of only 55 s, so this is not a problem. However, even in secular equilibrium ^{208}Tl does not have the same activity as ^{232}Th . In the decay series of ^{232}Th , ^{212}Bi undergoes beta decay to produce ^{208}Tl . The probability for this beta decay is 0.3594. Thus, one needs to multiply the gamma yield for ^{208}Tl to emit a 2614 keV gamma, which is 0.9975, by 0.3594. The product of these two probabilities, as shown in Table III, is the effective yield for the decay of ^{212}Bi to result in emission of a 2614 keV gamma.
- (3) An isolated photopeak is fitted well by a Gaussian function containing three parameters, a peak center, peak height, and peak width. To fit the spectral data, this Gaussian function needs to be added to a background function. The determination of the counts under the photopeak will to some extent depend on the choice of this background function and the range of channels for the fit, the fitting window, and hence add some systematic error. In our lab, we have written our own programs to guide students in determining the counts under a photopeak. Our choice of background function is described in Ref. 5.
- (4) Since the density of the KCl standard sample is different than the soil, the amount of self absorption will be different for the 1461 keV gamma in the KCl sample than the soil. In Appendix B, we develop a method to correct (approximately) S_{1461}^{KCl} for this effect. We note, that the product $S_{1461}^{\text{s}} \epsilon_{1461}$ is only needed if one wants to measure the absolute activity. The activity ratios are independent of $S_{1461}^{\text{s}} \epsilon_{1461}$. Also, another way to estimate $S_{1461}^{\text{s}} \epsilon_{1461}$ is to mix in a known amount of KCl uniformly in the sample.¹
- (5) As shown in Table III, there are two gammas emitted by ^{214}Bi , from the ^{238}U decay series, that have energies near 1764 keV. To account for the small amount of radiation from these two “side” gammas, we fit the spectrum near the 1764 keV photopeak with the sum of three gammas. The spectral height $S(i)$ as a function of channel number i for the 1764 keV photopeak is taken to be

$$S(i) = h \left(0.188 e^{(i-c_1)^2/2\sigma^2} + e^{(i-c_2)^2/2\sigma^2} + 0.133 e^{(i-c_3)^2/2\sigma^2} \right), \quad (5)$$

where h is the height, σ is the width, and c_2 is the channel number of the main 1764 keV photopeak. The numbers $c_1 = (1729.6/1764.5)c_2 \approx 0.98c_2$ and $c_3 = (1847.4/1764.5)c_2 \approx 1.047c_2$ correspond to the channel numbers of the two smaller side peaks scaled to the channel number of the main peak. The factors $0.188 = 0.0288/0.153$ and $0.133 = 0.0203/0.153$ are the ratio of the yields of the side peaks to the main peak. We have put this special fit for the 1764 keV photopeak into our curve fitting software.⁷ The 1461 keV and the 2614 keV gammas do not have any radiation within $\pm 3\sigma$ of their energies.

Table V. Comparison of the results for the activities A of the two soils using the NaI versus the Ge detector. The activities are in units of Bq, and the errors listed are statistical only.

Soil (Detector)	$A(^{238}\text{U series})$	$A(^{232}\text{Th series})$	$A(^{40}\text{K})$
Backyard (NaI)	22 ± 2	41 ± 2	925 ± 9
Backyard (Ge)	24 ± 3	44 ± 4	801 ± 46
Desert (NaI)	48 ± 2	42 ± 2	745 ± 10
Desert (Ge)	49 ± 4	47 ± 4	624 ± 41

- (6) It is not surprising that $\epsilon(E_\gamma)$ is approximately proportional to E_γ^b in the energy range which we consider. The photopeak is a result of electron photoabsorption in the NaI crystal. In Fig. 2.18 of Ref. 8, a log-log plot of the photoabsorption probability in NaI as a function of E_γ is close to a straight line in the energy range of 500 keV to 2000 keV. Self-absorption is a result of gamma scattering and absorption in the soil sample. The average mass attenuation coefficient of various soils also follows a power law relation with energy E_γ for energies between 122 keV and 1332 keV.⁹
- (7) The experiment can be simplified and only affect the results by 20% or so. One could use only the ^{207}Bi disk source to verify that $S^{\text{s}}(E)\epsilon(E)$ obeys a power law function and to determine the exponent b . One could fit the 1764 keV photopeak with a single Gaussian function and neglect the self-absorption correction for S_{1461}^{KCl} described in Appendix B. One can use b_{ave} for the exponent b instead of averaging b_{ave} and the value from Eq. (A2). With these modifications, the experiment is still a valuable exercise in detector calibration and measuring radiation in the environment.

IV. FINAL COMMENTS

For comparison, we list the results for the isotope activities as measured by the two types of detectors in Table V. From the table, we see that activities determined using the NaI detector are consistent with those from the Ge detector. The values from both detectors are in line with values for radioactive content in soils.¹⁰ Considering all errors, we would place an uncertainty of 15% for our NaI detector results.

There are other methods of calibrating the detector for a soil analysis. If one has a calibrated soil sample, with a known amount of potassium, ^{238}U , and ^{232}Th each in secular equilibrium, then one could compare unknown soil samples to the calibrated one. We could calibrate a soil sample with our Ge detector, and have students compare their measurements to this calibrated source. However, we find it more beneficial to run the experiment without a calibrated soil source and to have the students do the calibration themselves. By calibrating the detector for efficiency and sample absorption, the students also learn about the energy dependence of the gamma-electron interaction for gamma energies $500 < E_\gamma < 2700$ keV. We note that when measuring radiation in the field, other methods of calibration are used. In Ref. 11, a Window Analysis Method is used to instruct engineers in measuring gamma radiation in the environment.

ACKNOWLEDGMENT

The authors gratefully acknowledge the National Science Foundation support for R. Aguilar provided via the CSU-LSAMP program.

APPENDIX A: ESTIMATING THE EXPONENT B IN THE SOIL

The exponent b for the energy dependence of the product $S^s(E)\epsilon(E)$ is a critical parameter in comparing the detector's efficiency for the energies of the three gammas that are being measured in the soil. Using the disk sources, the students measure and confirm the power law function for this product for the energy range $511 \rightarrow 1770$ keV with the disk source behind the soil and with the soil removed. Let the exponent be b_0 without the soil and b_s with the soil present. We want to know the energy dependence of $S^s\epsilon$ for isotopes uniformly distributed in the soil. We label this exponent as b_{situ} , i.e., b *in situ*. A critical question is: how does one estimate b_{situ} from b_0 and b_s .

To help answer this question, we use our high resolution Ge detector, which can measure b_{situ} , to measure and compare the values of all the exponents: b_0 , b_s , and b_{situ} . Using the same procedure as with the NaI detector, we measured b_0 and b_s using the disk sources for each soil sample with the Ge detector. Then, we took a 20 h reading of just the soil sample, as in Ref. 1, to determine b_{situ} . In Fig. 5, we show a plot of the counts divided by the yield after subtracting background radiation for our backyard soil sample. The data are fit in the same manner as the disk source data, with a common exponent b and a separate activity for the ^{238}U and the ^{232}Th series.¹ As can be seen in the figure, the product $S^s(E)\epsilon(E)$ is to a good approximation proportional to $E^{-0.96}$ over the energy range $583 \rightarrow 2614$ keV, which is a remarkable result. In Table VI, we show the results of our measurements using the disk sources and the soil by itself.

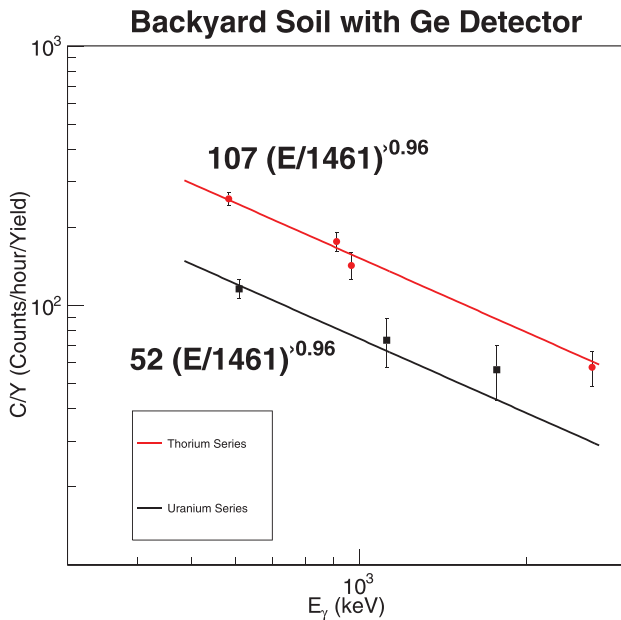


Fig. 5. Plot of Counts/Yield for the backyard soil taken with our high resolution Ge detector. The data for the plot were collected for 20 h. The log-log graph demonstrates that $S^s(E_\gamma)\epsilon(E_\gamma)$ is fairly well approximated by a power law relationship with $b_{\text{situ}} = -0.96$ for the energy range $583 \leq E_\gamma \leq 2614$ keV.

Table VI. The exponents b using the high resolution Ge detector. The first three rows are values obtained from the Counts/Yield measurements. The first two are from the disk source data: b_0 (no soil), b_s (with soil attenuation). The next one is the value b_{situ} for the two soils in the energy range $583 \leq E_\gamma \leq 2614$ keV. The last three rows are calculations using the average disk source values, Eqs. (A2) and (A3). The uncertainties listed are statistical only.

Exponent values	Backyard soil	Desert soil
b_0	-1.13 ± 0.01	-1.13 ± 0.01
b_s	-0.76 ± 0.02	-0.62 ± 0.02
$b_{\text{situ}} (583 \leq E \leq 2614)$	-0.96 ± 0.09	-0.89 ± 0.08
b_{ave}	-0.95 ± 0.02	-0.88 ± 0.02
b [Eq. (A2)]	-1.03	-0.99
b [Eq. (A3)]	-0.95	-0.89

One can also try and model the energy dependence of $S^s(E)$ and $\epsilon(E)$. The model we will take for the calculation is that the radiation from each part of the sample undergoes exponential attenuation before it reaches the detector, and that radiation hits perpendicular to the face of the detector. These assumptions are not perfect, since the sample is nearly a cube and not a cylinder whose cross section is the same size as the face of the detector. Also, radiation from each part of the sample has a different detector solid angle. However, although oversimplified the calculation can be followed by undergraduate students.

Let x be the distance from the center of the face of the detector to a point along the axis of the detector. First consider $\epsilon(E, x)dx$, which represents the detector efficiency for radiation emitted from a thin slab of thickness dx perpendicular to the axis without any material between the slab and detector that would absorb the radiation. From a previous experiment, the students have verified, using a disk source, that the efficiency for points on the axis of the detector is proportional to the solid angle: $\epsilon(x) \propto 1/(x+d)^2$, where d is the distance to an effective center of the detector. For our 2 in. NaI detector, $d \approx 3$ cm. Also, using the ^{207}Bi and ^{22}Na disk sources, we measured the exponent b_0 for different locations on the axis of the detector. Remarkably, b_0 hardly varied at all. Only near the detector was there any change. Right up against the detector, at $x=0$, $|b_0|$ was only 5% greater than at $x=9.2$ cm. From the results of these experiments, we model the energy dependence of ϵ for a source on the x -axis as

$$\epsilon(E, x) \propto \frac{E^{b_0}}{(x+d)^2}. \quad (\text{A1})$$

For the self-absorption factor S^s , the x dependence should be proportional to $e^{-\alpha x}$, where α is the linear attenuation constant. The energy dependence of S^s is contained in α : $S^s(E, x) \approx e^{-\alpha(E)x}$. The attenuation constant α has a strong energy dependence for $300 < E_\gamma < 2614$ keV. The disk source experiments gave $S^s(E, L)\epsilon(E, L) \propto E^{b_s}$. Thus, we have

$$\begin{aligned} S^s(E, L)\epsilon(E, L) &\propto E^{b_s} \\ e^{-\alpha(E)L}E^{b_0} &\propto E^{b_s} \\ e^{-\alpha(E)} &\propto E^{\delta_b/L}, \end{aligned}$$

Eqs. A2 and A3

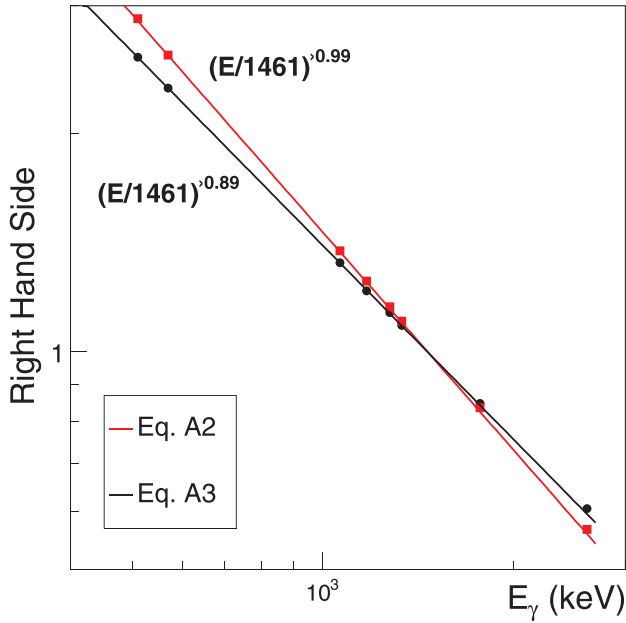


Fig. 6. Plots of the right hand sides of Eqs. (A2) and (A3) for the desert soil. Values used in the integral are $b_0 = -1.13$, $b_s = -0.62$, $d = 3$ cm, and $L = 9.2$ cm. The data points are calculated at the seven disk source energies plus $E = 2614$ keV, and are scaled so both integrals equal one at $E_\gamma = 1461$ keV.

where $\delta_b = b_s - b_0$. Putting all the pieces together, we obtain

$$\left(\frac{E}{1461}\right)^b \propto \left(\frac{E}{1461}\right)^{b_0} \int_0^L \left(\frac{L+d}{x+d}\right)^2 \left(\frac{E}{1461}\right)^{\delta_b x/L} \frac{dx}{L}, \quad (\text{A2})$$

as an approximate proportionality equation relating b_0 , b_s , and b . The self-absorption factor has the expected x dependence, and has the correct E dependence at $x=0$ and $x=L$. Equation (A2) needs to be solved numerically, but if $(L+d)^2/(x+d)^2$ is neglected, the integral has an analytical solution

$$\left(\frac{E}{1461}\right)^b \propto \frac{(E/1461)^{b_s} - (E/1461)^{b_0}}{\ln(E/1461)}, \quad (\text{A3})$$

where E is in units of keV.

To use Eqs. (A2) and/or (A3), one needs to pick energies between 511 and 2614 keV and evaluate and plot the right side of the equation. Then see if the resulting plots obey a power law, and if so determine the exponent b . In Fig. 6, we plot the calculations for the desert soil of the right sides of Eqs. (A2) and (A3) for the seven energies used with the disk sources plus $E = 2614$ keV, the energy from ^{208}Tl . The plots are scaled such that at $E = 1461$ keV the two calculations both equal one. From the figure, one sees that the right sides of Eqs. (A2) and (A3) are well fit by a power law function.

In Table VI, we list the values of the exponent b for the two soils. We are interested in estimating b_{situ} from the measurements of b_0 and b_s . As seen in the table, $b_{\text{ave}} = (b_0 + b_s)/2$ is very close to the *in situ* value for both soils. However, the statistical errors in measuring b_{situ} are quite large, around 10%. Radiation from the soil that is near the detector

should contribute more to the photopeaks, since it is closer to the detector and has a lower probability of being absorbed before entering the detector. Thus, one would expect the correct value for b to be closer to b_0 than to b_s , and lie in the range between b_{situ} and its lower statistical limit. The value of b from Eq. (A2) has this property, and is calculated using data from the NaI detector. Therefore, we believe that a reasonable estimate for the exponent b in the soil analysis lies between b_{ave} and the value from Eq. (A2): $b_{\text{ave}} > b > b$ [Eq. (A2)]. For both the backyard and desert soils, the best estimate for b is 5% more negative than b_{ave} , with an uncertainty of 5%.

APPENDIX B: SELF-ABSORPTION CORRECTION FOR S_{1461}^s

The calibration factor $S_{1461}^{\text{KCl}} \epsilon_{1461}$ is determined from the spectrum of a sample of pure KCl. However, what we need for the soil sample “s” is the product $S_{1461}^s \epsilon_{1461}$. Usually, the soil sample will not have the same density as the KCl sample. Generally, a more dense sample will absorb more radiation and result in a smaller value for S_{1461}^s . In this Appendix, we present a formula to approximate the ratio $(S_{1461}^s)/(S_{1461}^{\text{KCl}})$. Although the correction is not large, it is useful for the student to be aware of this effect.

The model we will take for the calculation is the same one we used in Appendix A: that the radiation from each part of the sample undergoes linear attenuation before it reaches the detector, and that radiation hits perpendicular to the face of the detector. Let A_{KCl} be the activity of ^{40}K in the KCl sample, and Y the gamma yield. Assuming linear attenuation, the rate of 1461 keV gammas, R , that reach the detector is

$$R_{\text{KCl}} \approx A_{\text{KCl}} Y \int_0^L e^{-\alpha x} (dx/L), \quad (\text{B1})$$

where R and A have the same dimensions of $(\text{time})^{-1}$, α is the linear attenuation constant for a 1461 keV gamma, and L is the length of the sample. The probability for the gamma to be scattered or absorbed before reaching the detector is roughly proportional to the electron density of the sample. Hence, the linear attenuation coefficient, α , is roughly proportional to the density, ρ , of the sample

$$R_{\text{KCl}} \approx A_{\text{KCl}} Y \int_0^L e^{-\mu x \rho_{\text{KCl}}} (dx/L), \quad (\text{B2})$$

where $\mu = \alpha/\rho$ is called the mass attenuation coefficient evaluated at $E_\gamma = 1461$ keV. There is no energy dependence in the integral. Evaluating the integral gives

$$R_{\text{KCl}} \approx \frac{A_{\text{KCl}} Y}{\mu L \rho_{\text{KCl}}} (1 - e^{-\mu L \rho_{\text{KCl}}}), \quad (\text{B3})$$

where ρ_{KCl} is the density of the KCl sample. However, we need the rate R_{soil} of gammas reaching the detector if the activity of ^{40}K is A_{KCl} but the density of the KCl sample is ρ_{soil} , i.e., equal to the soil sample

$$R_{\text{soil}} \approx \frac{A_{\text{KCl}} Y}{\mu L \rho_{\text{soil}}} (1 - e^{-\mu L \rho_{\text{soil}}}). \quad (\text{B4})$$

The ratio $R_{\text{soil}}/R_{\text{KCl}}$ is the ratio of the self-absorption factors S_{1461}^{soil} and S_{1461}^{KCl} . Taking the ratio of the two equations gives

Table VII. Self absorption correction data using Eq. (B8). The mass of the KCl salt sample was $m_{\text{KCl}} = 863$ g.

Sample	Mass (g)	f	$(S_{1461}^{\text{S}})/(S_{1461}^{\text{KCl}})$
Backyard soil	1300	0.61	0.93
Desert soil	1790	0.42	0.82

$$\frac{S_{1461}^{\text{S}}}{S_{1461}^{\text{KCl}}} = \frac{R_{\text{soil}}}{R_{\text{KCl}}} \approx \frac{\rho_{\text{KCl}} (1 - e^{-\mu L \rho_{\text{soil}}})}{\rho_{\text{soil}} (1 - e^{-\mu L \rho_{\text{KCl}}})}. \quad (\text{B5})$$

To eliminate the product μL , we can use data taken with the disk sources. The ratio of the counts from a disk source with and without the soil in the way is equal to $e^{-\mu L \rho_{\text{soil}}}$. We define the ratio f as $f \equiv (\text{counts with soil})/(\text{counts without soil})$ emitted from a disk source for a gamma energy of 1461 keV. From our disk source analysis, we f is equal to the ratio: $f = C_{\text{D1461Y1}}(\text{with soil})/C_{\text{D1461Y1}}(\text{without soil})$. Thus,

$$f = \frac{C_{\text{D1461Y1}}(\text{with soil})}{C_{\text{D1461Y1}}(\text{without soil})} = e^{-\mu L \rho_{\text{soil}}}, \quad (\text{B6})$$

where D can be any one of the three disk sources. Replacing $e^{-\mu L \rho_{\text{soil}}}$ with f in Eq. (B5), we have

$$\frac{S_{1461}^{\text{S}}}{S_{1461}^{\text{KCl}}} \approx \frac{\rho_{\text{KCl}}}{\rho_{\text{soil}}} \left(\frac{1 - f}{1 - f(\rho_{\text{KCl}}/\rho_{\text{soil}})} \right). \quad (\text{B7})$$

Since the volumes of all the soil and KCl samples are the same, we use the mass of the samples in our calculations

$$\frac{S_{1461}^{\text{S}}}{S_{1461}^{\text{KCl}}} \approx \frac{m_{\text{KCl}}}{m_{\text{soil}}} \left(\frac{1 - f}{1 - f(m_{\text{KCl}}/m_{\text{soil}})} \right), \quad (\text{B8})$$

where the fraction f can be determined from any one of the three disk sources.

To show the effect of correcting for self absorption in the calibration constant, we list in Table VII the results for two soils with different densities. One sample is from a local backyard, and the other is from a desert in Nevada.

Instead of using Eq. (B8), another option is to estimate the attenuation of a 1461 keV gamma through the KCl sample. If we define f_{KCl} as

$$f_{\text{KCl}} = \frac{C_{\text{Bi1461Y1}}(\text{with KCl})}{C_{\text{Bi1461Y1}}(\text{without KCl})} = e^{-\mu L \rho_{\text{KCl}}}, \quad (\text{B9})$$

then Eq. (B5) becomes

$$\frac{S_{1461}^{\text{S}}}{S_{1461}^{\text{KCl}}} \approx \frac{\rho_{\text{KCl}}}{\rho_{\text{soil}}} \left(\frac{1 - f}{1 - f_{\text{KCl}}} \right). \quad (\text{B10})$$

Due to the presence of the 1461 keV photopeak from the KCl sample, ^{207}Bi is the most reliable disk source to use to estimate f_{KCl} .

^aElectronic mail: pbsiegel@cpp.edu

¹P. B. Siegel, "Gamma spectroscopy of environmental samples," *Am. J. Phys.* **81**, 381–388 (2013).

²Data acquisition with the 2-inch NaI gamma detector is done with Digibase from Ortec. The acquisition software produces a 1024 channel *.Chn file, which we read and analyze with our own software.

³The isotope decay data and disk source data were obtained from the National Nuclear Data Center at Brookhaven National Laboratory. The data are available at the following web site: <<https://www.nndc.bnl.gov/nudat2/>>.

⁴The link to obtain the exponent b from the disk source data is found on our laboratory web page and is <<https://www.cpp.edu/~pbsiegel/javascript/disksources.html>>. The app initially gives the linear regression result, then an option to do a chi-square analysis.

⁵Byron Curry, Dave Riggins, and P. B. Siegel, "Data analysis in the undergraduate nuclear laboratory," *Am. J. Phys.* **63**, 71–76 (1995).

⁶John R. Taylor, *An Introduction to Error Analysis*, 2nd ed. (University Science Books, California, 1997). After taking the logarithm of both sides of Eq. (3), we use the methods of Chap. 8 to solve for the common slope b and the three C_{D1461Y1} values.

⁷We solve for the minimum of the function $\chi^2 \equiv \sum_i^7 (C_i - Y_i C_{\text{D1461Y1}} (E/1461)^b)^2 / C_i$ to determine b and the three C_{D1461Y1} values. The software the students use is found and explained on our laboratory manual for the Radiation Laboratory Course at <<https://www.cpp.edu/~pbsiegel/phy432/labman/manual.html>>.

⁸G. F. Knoll, *Radiation Detection and Measurement*, 3rd ed. (Wiley, New York, 1999). See Fig. 2.18 for a plot of the energy dependence of gamma-ray interaction processes in sodium iodide.

⁹M. S. Al-Masri, M. Hasan, A. Al-Hamwi, Y. Amin, and A. W. Doubal, "Mass attenuation coefficients of soil and sediment samples using gamma energies from 46.5 to 1332 keV," *J. Environ. Radioactivity* **116**, 28–33 (2013).

¹⁰Typical values for ^{232}Th and ^{238}U in soils range between 15 and 60 Bq/kg. See Kekelidze *et al.*, "Radioactivity of soils in Mtskheta-Myianeti region (Georgia)," *Ann. Agrarian Sci.* **15**, 304–311 (2017) for a detailed analysis of soils in Georgia.

¹¹Alberi *et al.*, "Training future engineers to be ghostbusters: Hunting for the spectral environmental radioactivity," *Educ. Sci.* **9**(1), 1–14 (2019).